A novel numerical approach to Fluid-Structure interaction problem.

by

Rahim Usubov

A thesis submitted in partial fulfillment of the requirements for the degree of

Master of Science

in

Applied Mathematics

Department of Mathematical and Statistical Sciences
University of Alberta

Abstract

This work develops numerical methods (finite difference methods) for equations of fluid dynamics and equations of elasticity reformulated in the stress variables (as opposed to natural variables) and applies them to the Fluid-Structure Interaction (FSI) problem using a new model based on the level set method. Equations reformulated in stress variables are the stress formulation. Previously some work has been done on numerical methods for stress formulation for the Navier-Stokes equation. This work extends this research to the equations of elasticity. Additionally the current research develops a new model for FSI problems are based on this stress formulation and the level set method. Using this model and new numerical method for FSI problems is developed with some constraints. Some benchmark results are presented.

Table of Contents

List of Figures

List of Notations.

δ_{ij}	Kronecker delta
v_i	velocity
u_i	displacement
σ_{ij}	stress tensor
p	pressure
f_i	external force
ϕ	level set function
ρ^f, ρ^s	fluid/structure density
μ^f	fluid viscosity
μ^s	structure elasticity
ψ^n	quantity ψ discretized in time at level n
$\delta\psi^n$	first finite difference in time: $\delta\psi^n = \psi^n - \psi^{n-1}$
$\delta^2\psi^n$	second finite difference in time: $\delta^2\psi^n = \delta\psi^n - \delta\psi^{n-1}$
τ	step size in time
h	step size in space
d	number of spacial dimensions

Chapter 1

Introduction

The fluid-structure interaction (FSI) problem describes the mechanical interaction of a fluid and an elastic solid. This problem requires the simultaneous use of different models to describe the fluid and the elastic structure media as well as tracking the interface that couples these media and impose appropriate boundary conditions. This also involves solving equations of the corresponding models in changing over time domains. The fact that fluid equations are usually formulated the Eulerian framework, while the elasticity problems are considered from the Lagrangian perspective poses another challenge. This problem has numerous applications in medicine and engineering, such as blood flow in heart or flexible blood vessels, flow induced vibrations in various structures and bio-mechanics [Hou *et al.* 2012], [Hoffman *et al.* 2011].

Let us summarize some of the previously successful methods used to solve this problem.

The simplest approach is called partitioned methods. In this case, fluid and elasticity solvers are used to solve the fluid and structure problems separately. The solutions matched using the boundary conditions at the fluid-structure interface

iteratively. Advantages of this approach are simplicity of the core idea and ability to reuse fluid and elasticity solvers developed earlier [Hou *et al.* 2012], [Dunne 2006].

Another approach that has been widely studied is based on the Arbitrary Lagrange-Eulerian formulation (ALE) [Hron & Turek 2006]. The core idea of the method is to describe the motion of elastic or fluid medium in a moving reference frame, which is not necessarily tied to the actual motion of fluid or structure. In ALE solver for FSI problems, the Lagrange formulation is usually used for structure and interface motion. This is one of the monolithic descriptions. Fluid and structure are treated within the same framework. A mapping is introduced between the reference configuration and the domain configuration at current time. It is natural to use the initial configuration as the reference configuration in the structure subdomain. Since structure is described in Lagrange framework, this mapping transforms the initial configuration of the solid to the configuration at the current time, thus it is related to the structure displacements. The corresponding mapping in the fluid may become complicated, so a simpler relation for displacements in the fluid domain is used to define this mapping. Fluid and structure equations are reformulated using this mapping. Once the weak formulation is written, the equations are transformed into the reference configuration and a finite element discretization is derived. Thus, the complex problem of evolution of fluid-structure interface over time is solved. The boundary conditions are taken into account naturally, when writing the weak formulation. The velocity is continuous across the interface, The force balance condition on the interface is described by the difference of the surface integrals. By omitting these surface integrals in the resulting formulation, the stress interface condition is imposed implicitly. The resulting non-linear system is solved using the Newton method. This idea of representing the fluid and structure as in a unified medium and solving the problem in the reference configuration is also studied in

[Le Tallec & Mouro 2001]. Additional attention is given to the discretization of the problem, solving elastic shell models and general advantages of such approaches.

The ALE treatment of a special phase field function used to distinguish the fluid and structure media is presented in [Hoffman *et al.* 2011]. This phase field function defines the material properties and constitutive laws. However, the equations of motion are formulated in Euler coordinates.

Another hybrid method (Eulerian-Lagrangian) is presented in [Legay *et al.* 2006]. In this method there is no need for updating the fluid mesh. Fluid and structure equations of motion are formulated in Euler frame and combined into a single weak formulation using a smoothed Heaviside function, zero in one subdomain and one in the other. A signed distance level set function is used to distinguish the subdomains. Additionally, Lagrange multipliers are introduced to the weak formulation to explicitly impose the velocity and stress boundary conditions.

A method based on a fully Eulerian formulation for both fluid and elastic structure has been developed in [Dunne 2006], [Dunne & Rannacher 2006]. After reformulation, the weak formulation is considered. In this framework, the boundary conditions at the fluid-structure interface are treated implicitly: after integration by parts, the surface integrals are omitted implying the correct boundary conditions similar to [Hron & Turek 2006]. An additional function which plays the role of a phase variable is used to distinguish between fluid and structure. An approach analogous the the level set method is used to transport this function and keep track of the initial positions of all structure points in the Eulerian perspective. The velocity used to advect this phase function is the structure velocity in the structure and a harmonic continuation to the fluid subdomain outside of structure. This is also similar to the idea in [Hron & Turek 2006]. As a result of this approach, an intermediate step for the phase function in unnecessary. This also preserves the corners and edges of the

structure domain.

Another class of methods is immersed methods, that have emerge from the immersed boundary method first proposed in [Peskin 1977] to describe blood flow in a heart. The immersed boundary method describes the motion of an elastic fiber in a fluid. These methods assume that the structure domain is filled with the same fluid. The fluid-structure interaction forces are computed using the equation of motion for the structure and applied the fluid in the structure domain. Then, the fluid equations are solved with this interaction force taken into account. The structure velocity is set to be the fluid velocity in the structure domain. The location of the fluid-structure interface is updated using the velocity of the structure [Hou *et al.* 2012].

Let us describe the mathematical setting for the FSI problems. Domain Ω is partitioned into two subdomains Ω^f and Ω^s. The fluid-structure interface is Γ (Fig. 1.1).

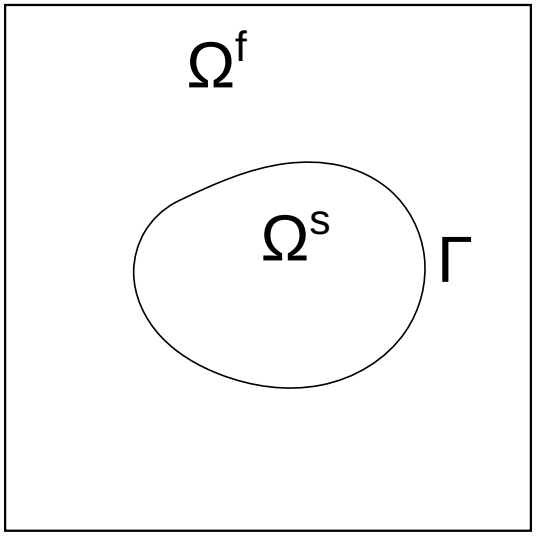

Figure 1.1: Problem setting.

The motion of the fluid in the fluid domain Ω^f is governed by the equation of motion and incompressibility condition. The formulation is usually given in the

Euler frame (we assume Einstein summation notation):

$$\begin{aligned} &\partial_t v_i + v_k \partial_k v_i - \frac{\partial_k \sigma^f_{ik}}{\rho^f} = \frac{f_i}{\rho^f}; \\ &\partial_k v_k = 0; \\ &\sigma^f_{ij} = \mu^f \left(\partial_i v_j + \partial_j v_i\right) - \delta_{ij} p. \end{aligned} \tag{1.1}$$

Here v_i is the fluid velocity, σ^f_{ik} is the fluid stress tensor, f_i is the external force, p is the fluid pressure, parameters μ^f and ρ^f are the fluid viscosity and density respectively.

The motion of the elastic structure in Ω^s is governed by the equation of motion of linear elasticity and incompressibility condition. The formulation is usually given in the Lagrange frame:

$$\begin{aligned} &\frac{dv_i}{dt} - \frac{\partial_k \sigma^s_{ik}}{\rho^s} = \frac{f_i}{\rho^s}; \\ &\partial_t u_i = v_i; \\ &\partial_k u_k = 0; \\ &\sigma^s_{ij} = \mu^s \left(\partial_i u_j + \partial_j u_i\right) - \delta_{ij} p. \end{aligned} \tag{1.2}$$

Here v_i is the structure velocity, σ^s_{ik} is the elastic stress tensor, f_i is the external force, p is the structure pressure, parameters μ^s and ρ^s are the solid lame parameter (shear modulus) and density respectively. The shear modulus is connected to the Young modulus E and the Poisson ratio σ : $\mu = \frac{E}{2(1+\sigma)}$. Note the full time derivative $\frac{dv_i}{dt}$.

We assume linear incompressible elastic stress tensor. We will reformulate these equations in the Euler frame.

The boundary conditions are imposed on the interface Γ:

$$\begin{aligned} \sigma^s_{ik} n_k &= \sigma^f_{ik} n_k, \quad \Gamma; \\ v_i &= \partial_t u_i, \quad \Gamma. \end{aligned} \tag{1.3}$$

Here, n_i is the unit normal vector to Γ. These conditions are formulated in the Euler frame and higher order terms (in u_i, v_i) are neglected.

The aim of this research is to reformulate the original equations of motions into a stress formulation. Using this formulation we will be able to develop a regularized approximation using the level set method. Finally we will develop a numerical method to solve the new regularized stress formulation for the fluid-structure interaction.

Chapter 2

The Stress Formulation.

In this section we review a numerical study done previously on the stress formulation, and extend it in order to describe the FSI problem.

2.A Previous Studies.

The formulation of equations of elasticity in terms of stress components (the stress formulation) has been proposed in [Konovalov 1997]. Further numerical development has been carried out in [Minev & Vabishchevich 2018] and a potential application of this formulation for the FSI problem is noted. Since the stress formulation is an important part of this study, let us summarize the development of numerical schemes for the stress formulation in context of Navier-Stokes equations.

The stress formulation is derived by taking the gradient of the original equations of motion in terms of velocities and pressure. In [Minev & Vabishchevich 2018] time dependent Stokes and Navier-Stokes are considered with the gradient-stress tensor for incompressible flow, instead of the symmetric stress. This results in 4 equations in two dimensional case for all the components of stress. To deal

with the resulting system a time-splitting scheme is introduced. The off-diagonal components of stress are split from the diagonal components. The stability of such time-splitting scheme is studied analytically. Additionally, two different ways of decoupling and solving discretized diagonal equations are introduced. One way is to transform the resulting linear system and apply direction splitting. The other way is to split one diagonal component from the other, using it explicitly in one of the diagonal equations. Both methods result in tridiagonal linear systems which can be solved with optimal performance. Thus, all components of the gradient-stress are computed. To find the velocities, one may use the computed gradient stress in the original equations of motion in natural variables. The article also extends these schemes to include the convection terms of the Navier-Stokes equations. These non-linear terms are included explicitly in the scheme. The possibility of extending the scheme to the symmetric stress tensor is discussed.

Since this work is based on and extends the results of [Minev & Vabishchevich 2018], let us summarize a part of the derivation of the numerical scheme performed there. Starting with the velocity v_i and pressure p defined on a time interval $[0;T]$ and in open domain Ω we write the equations of motion along with the incompressiblity condition:

$$\begin{cases} \partial_t v_i - \partial_k \left(\nu \partial_k v_i\right) + \partial_i p = f_i; \\ \partial_i v_i = 0. \end{cases} \tag{2.1}$$

Here f_i is the external force, ν is the kinematic viscosity ($\nu = \frac{\mu}{\rho}$, μ is viscosity and ρ is density of the fluid).

To transform this equation into a stress formulation we define the gradient stress

$$\sigma_{ij} = \nu \partial_j v_i - \delta_{ij} p. \tag{2.2}$$

Taking the gradient of the first equation in 2.1 we get the following system:

$$\partial_t \left(\frac{\sigma_{ij}}{\nu} \right) + \partial_t \left(\frac{\delta_{ij} p}{\nu} \right) = \partial_j \partial_k \sigma_{ik} + \partial_j f_i. \tag{2.3}$$

From 2.2 we derive a new form of the incompressibility conditions, using the original incompressibility condition (second equation of 2.1:

$$p = -\frac{1}{d} \sigma_{ii}, \tag{2.4}$$

where d is the number of spacial dimensions. Substituting this form of incompressibility condition, we get the following stress formulation:

$$\partial_t \left(A_{ijlm} \sigma_{lm} \right) = \nu \left(\partial_j \partial_k \sigma_{ik} + \partial_j f_i \right). \tag{2.5}$$

Here, $A_{ijlm} = \delta_{il}\delta_{jm} - \frac{1}{d}\delta_{ij}\delta_{lm}$. The boundary conditions for 2.5 on $\partial\Omega$ are:

$$\left(\partial_k \sigma_{ik} \right) n_j = \left(\partial_t v_i - f_i \right) n_j, \tag{2.6}$$

with n_i being the outward normal to the $\partial\Omega$. Once the equations 2.5 are solved for σ_{ij}, the velocity can be computed from the original equations of motion 2.1.

The system 2.5 includes 4 equations for 4 unknowns σ_{ij} in two dimensions. To simplify the resulting scheme after discretizing in time, time splitting is used. This is done so that equations for diagonal components of stress can be solved separately from the equations for off-diagonal components. For this, the diagonal components in the off-diagonal equations are taken explicitly. The first order in time version of

the time-splitting scheme can be formally written:

$$\delta\left(A_{ijlm}\delta\sigma_{lm}^{n+1}\right)-\nu\tau\left(\partial_j\partial_k\sigma_{ik}^{n+1}-D(\delta\sigma_{ik}^{n+1})\right)=\nu\tau\partial_j f_i^{n+1}, \tag{2.7}$$

with operator $D(\delta\sigma_{ik}^{n+1})$ defined as:

$$D(\delta\sigma_{ik}^{n+1})=\begin{pmatrix}0 & \partial_2\partial_1\delta\sigma_{11}^{n+1}\\ \partial_1\partial_2\delta\sigma_{22}^{n+1} & 0\end{pmatrix}. \tag{2.8}$$

In components the discretized in time system is written:

$$\begin{cases}\delta\sigma_{12}^{n+1}-\nu\tau\left(\partial_2\partial_2\sigma_{12}^{n+1}+\partial_2\partial_1\sigma_{11}^{n}\right)=\nu\tau\partial_2 f_1^{n+1}\\ \delta\sigma_{21}^{n+1}-\nu\tau\left(\partial_1\partial_1\sigma_{21}^{n+1}+\partial_1\partial_2\sigma_{22}^{n}\right)=\nu\tau\partial_1 f_2^{n+1}\\ \delta\left(\sigma_{11}-\sigma_{22}\right)^{n+1}-2\nu\tau\left(\partial_1\partial_1\sigma_{11}^{n+1}+\partial_1\partial_2\sigma_{12}^{n+1}\right)=\nu\tau\partial_1 f_1^{n+1}\\ \delta\left(\sigma_{22}-\sigma_{11}\right)^{n+1}-2\nu\tau\left(\partial_2\partial_2\sigma_{22}^{n+1}+\partial_2\partial_1\sigma_{21}^{n+1}\right)=\nu\tau\partial_2 f_2^{n+1}\end{cases} \tag{2.9}$$

This way we can first solve the equations for the off-diagonal components first and then use this result to solve for diagonal components.

2.B Extension of the Stress Formulation.

2.B.1 Symmetric stress.

In order to better represent the physical fluid and structure equations of motion, one must consider the symmetric stress instead of the gradient stress. With the linear stress-strain relation, the stress tensors for fluid σ_{ij}^f and structure σ_{ij}^s will read:

$$\begin{aligned}\sigma^f_{ij} &= \mu^f \left(\partial_i v_j + \partial_j v_i\right) - \delta_{ij} p,\\ \sigma^s_{ij} &= \mu^s \left(\partial_i u_j + \partial_j u_i\right) - \delta_{ij} p.\end{aligned} \tag{2.10}$$

Let us consider the derivation for a fluid model without the convection terms.

$$\partial_t v_i - \frac{\partial_k \sigma^f_{ik}}{\rho^f} = \frac{f_i}{\rho^f}. \tag{2.11}$$

The derivation for structure equations is similar. Following the derivation of analogous equations for gradient stress 2.5 in [Minev & Vabishchevich 2018] we take the gradient of this equation of motion:

$$\partial_t \partial_j v_i - \partial_j \left(\frac{\partial_k \sigma^f_{ik}}{\rho^f}\right) = \partial_j \left(\frac{f_i}{\rho^f}\right). \tag{2.12}$$

To obtain the symmetric strain tensor for fluid under the time derivative, we add the same equation transposed to this equation:

$$\partial_t \left(\partial_j v_i + \partial_i v_j\right) - \partial_j \left(\frac{\partial_k \sigma^f_{ik}}{\rho^f}\right) - \partial_i \left(\frac{\partial_k \sigma^f_{jk}}{\rho^f}\right) = \partial_j \left(\frac{f_i}{\rho^f}\right) + \partial_i \left(\frac{f_j}{\rho^f}\right). \tag{2.13}$$

Now, the strain tensor $\left(\partial_j v_i + \partial_i v_j\right) = \frac{1}{\mu^f}\left(\sigma^f_{ij} + \delta_{ij} p\right)$ is under the time derivative in the left hand side, and using the incompressibility condition $\partial_k v_k = 0$ rewritten in terms of stress and pressure(2.4) we can write the stress formulation:

$$\begin{aligned}&\frac{1}{\mu^f}\partial_t \left(A_{ijlm}\sigma^f_{lm}\right) - \partial_j \left(\frac{\partial_k \sigma^f_{ik}}{\rho^f}\right) - \partial_i \left(\frac{\partial_k \sigma^f_{jk}}{\rho^f}\right)\\ &= \partial_j \left(\frac{f_i}{\rho^f}\right) + \partial_i \left(\frac{f_j}{\rho^f}\right).\end{aligned} \tag{2.14}$$

Here, $A_{ijlm} = \delta_{ij}\delta_{lm} - \frac{1}{d}\delta_{il}\delta_{jm}$. We can apply the same time splitting 2.8 as

described in [Minev & Vabishchevich 2018], which will result in a first-order time discretization. Writing the system in components:

$$\begin{cases} \delta\sigma_{12}^{f,n+1} - \mu^f\tau\left(\Delta_{22}+\Delta_{11}\right)\sigma_{12}^{f,n+1} - \mu^f\tau\Delta_{21}\sigma_{11}^{f,n} \\ -\mu^f\tau\Delta_{12}\sigma_{22}^{f,n} = \mu^f\tau\partial_1\left(\dfrac{f_2^{n+1}}{\rho^f}\right) + \mu^f\tau\partial_1\left(\dfrac{f_2^{n+1}}{\rho^f}\right); \\ \\ \delta\left(\sigma_{11}^{f,n+1} - \sigma_{22}^{f,n+1}\right) - 4\mu^f\tau\Delta_{11}\sigma_{11}^{f,n+1} - 4\mu^f\tau\Delta_{12}\sigma_{12}^{f,n+1} \\ = 4\mu^f\tau\partial_1\left(\dfrac{f_1^{n+1}}{\rho^f}\right); \\ \\ \delta\left(\sigma_{22}^{f,n+1} - \sigma_{11}^{f,n+1}\right) - 4\mu^f\tau\Delta_{22}\sigma_{22}^{f,n+1} - 4\mu^f\tau\Delta_{21}\sigma_{21}^{f,n+1} \\ = 4\mu^f\tau\partial_2\left(\dfrac{f_2^{n+1}}{\rho^f}\right); \end{cases} \tag{2.15}$$

Here, $\Delta_{ij} = \partial_i \frac{1}{\rho^f}\partial_j$.

2.B.2 Structure equations.

The equations for a linear elastic incompressible structure are derived in a similar way as above. We start with the elasticity equations with linear stress tensor:

$$\begin{cases} \rho^s\partial_{tt}u_i - \partial_k\sigma_{ik}^s = f_i, \\ \sigma_{ij}^s = \mu^s\left(\partial_i u_j + \partial_j u_i\right) - \delta_{ij}p. \\ \partial_k u_k = 0. \end{cases} \tag{2.16}$$

Let us note that in general, the incompressibility condition for structure looks more complicated, but once we omit all except the linear terms (in the framework of linear elasticity), we get the simple condition mentioned above. Following the same procedure as in the previous subsection, we derive the structure stress formulation:

$$\begin{aligned} &\frac{1}{\mu^s}\partial_{tt}\left(A_{ijlm}\sigma^s_{lm}\right) - \partial_j\left(\frac{\partial_k\sigma^s_{ik}}{\rho^s}\right) - \partial_i\left(\frac{\partial_k\sigma^s_{jk}}{\rho^s}\right) \\ &= \partial_j\left(\frac{f_i}{\rho^s}\right) + \partial_i\left(\frac{f_j}{\rho^s}\right). \end{aligned} \tag{2.17}$$

These two advancements along with the regularized formulation will be used to derive a numerical scheme for FSI problems.

2.B.3 Convection terms.

For certain applications, like physiological flows [Sugiyama *et al.* 2017], it is reasonable to assume that fluid and structure densities are equal. In such case, we can incorporate the convection terms in the stress tensor:

$$\tilde{\sigma}^f_{ij} = \sigma^f_{ij} - \rho^f v_i v_j \tag{2.18}$$

In this case, the Navier-Stokes equations

$$\partial_t v_i + v_k\partial_k v_i - \frac{\partial_k\sigma^f_{ik}}{\rho^f} = \frac{f_i}{\rho^f} \tag{2.19}$$

can be rewritten using the incompressibility conditions using the new stress tensor:

$$\partial_t v_i - \frac{\partial_k\tilde{\sigma}^f_{ik}}{\rho^f} = \frac{f_i}{\rho^f} \tag{2.20}$$

The structure equations can be reformulated the same way. In the structure the term $v_i v_j$ will be negligible due to the assumption of linear elasticity.

The stress formulation is straightforward to derive. We follow the same procedure as for 2.14 except for an additional term under the time derivative. The system reads:

$$\begin{aligned}&\frac{1}{\mu^f}\partial_t\left(A_{ijlm}\tilde{\sigma}^f_{lm}\right)+\frac{1}{\mu^f}\partial_t\left(A_{ijlm}\rho^f v_l v_m\right)\\&-\partial_j\left(\frac{\partial_k\tilde{\sigma}^f_{ik}}{\rho^f}\right)-\partial_i\left(\frac{\partial_k\tilde{\sigma}^f_{jk}}{\rho^f}\right)=\partial_j\left(\frac{f_i}{\rho^f}\right)+\partial_i\left(\frac{f_j}{\rho^f}\right).\end{aligned}\tag{2.21}$$

Discretization follows the same procedure as for the 2.14, the derivative $\partial_t\left(A_{ijlm}\rho^f v_l v_m\right)$ can be approximated explicitly. Due to this new term that depends on velocities, it becomes necessary to integrate velocities as well.

Chapter 3

Regularized formulation.

Here we develop the regularized formulations for the equations in terms of stress to treat the fluid-structure interface in the FSI problem. After a short setup, we will consider the conservative level set method that will be used in this formulation and apply it to the stress formulation derived earlier.

3.A Model of the Fluid-Structure interaction.

We assume that the domain of the problem Ω is divided into two subdomains: fluid Ω^f and structure Ω^s separated by a fluid-structure interface Γ. The motion of the fluid is described by the following governing equations:

$$\begin{cases} \partial_t v_i - \dfrac{\partial_k \sigma^f_{ik}}{\rho^f} = \dfrac{f_i}{\rho^f}, \\ \sigma^f_{ij} = \mu^f \left(\partial_i v_j + \partial_j v_i\right) - \delta_{ij} p, \\ \partial_k v_k = 0. \end{cases} \tag{3.1}$$

The motion of the structure is described by the following governing equations:

$$\begin{cases} \rho^s \partial_{tt} u_i - \partial_k \sigma^s_{ik} = f_i, \\ \sigma^s_{ij} = \mu^s \left(\partial_i u_j + \partial_j u_i \right) - \delta_{ij} p. \\ \partial_k u_k = 0. \end{cases} \tag{3.2}$$

Additionally we have interface boundary conditions on Γ. Here, we will denote the medium velocity in Ω^f as v^f_i, in Ω^s as v^s_i, vector n_i is the normal to Γ outward to Ω^s:

$$\begin{cases} \sigma^s_{ik} n_k|_\Gamma = \sigma^f_{ik} n_k \Big|_\Gamma, \\ v^s_i|_\Gamma = v^f_i \Big|_\Gamma. \end{cases} \tag{3.3}$$

Let us note that $v^s_i = \partial_t u_i$ in Ω^s.

Using the results from the previous chapter, we can reformulate these problems in terms of stress variables:

$$\begin{cases} \dfrac{1}{\mu^s} \partial_{tt} \left(A_{ijlm} \sigma^s_{lm} \right) - \partial_j \left(\dfrac{\partial_k \sigma^s_{ik}}{\rho^s} \right) - \partial_i \left(\dfrac{\partial_k \sigma^s_{jk}}{\rho^s} \right) \\ = \partial_j \left(\dfrac{f_i}{\rho^s} \right) + \partial_i \left(\dfrac{f_j}{\rho^s} \right), \quad \Omega^s; \\ \\ \dfrac{1}{\mu^f} \partial_t \left(A_{ijlm} \sigma^f_{lm} \right) - \partial_j \left(\dfrac{\partial_k \sigma^f_{ik}}{\rho^f} \right) - \partial_i \left(\dfrac{\partial_k \sigma^f_{jk}}{\rho^f} \right) \\ = \partial_j \left(\dfrac{f_i}{\rho^f} \right) + \partial_i \left(\dfrac{f_j}{\rho^f} \right), \quad \Omega^f. \end{cases} \tag{3.4}$$

With the convection terms this system will be:

$$\begin{cases} \dfrac{1}{\mu^s}\partial_{tt}\left(A_{ijlm}\tilde{\sigma}^s_{lm}\right) + \dfrac{1}{\mu^s}\partial_{tt}\left(A_{ijlm}\rho^s v_l v_m\right) - \partial_j\left(\dfrac{\partial_k\tilde{\sigma}^s_{ik}}{\rho^s}\right) - \partial_i\left(\dfrac{\partial_k\tilde{\sigma}^s_{jk}}{\rho^s}\right) \\ = \partial_j\left(\dfrac{f_i}{\rho^s}\right) + \partial_i\left(\dfrac{f_j}{\rho^s}\right), \quad \Omega^s; \\ \\ \dfrac{1}{\mu^f}\partial_t\left(A_{ijlm}\tilde{\sigma}^f_{lm}\right) + \dfrac{1}{\mu^f}\partial_t\left(A_{ijlm}\rho^f v_l v_m\right) - \partial_j\left(\dfrac{\partial_k\tilde{\sigma}^f_{ik}}{\rho^f}\right) - \partial_i\left(\dfrac{\partial_k\tilde{\sigma}^f_{jk}}{\rho^f}\right) \\ = \partial_j\left(\dfrac{f_i}{\rho^f}\right) + \partial_i\left(\dfrac{f_j}{\rho^f}\right), \quad \Omega^f. \end{cases} \tag{3.5}$$

Now, using this result and the level set method we will derive a regularized formulation.

3.B The level set method.

The level set method, introduced in [Osher & Sethian 1988] describes the interface in terms of a smooth level set function. The function is defined on the whole domain, its 0 or 0.5 level set (depending on the method) defines the interface. Often, the level set function is initialized to be a distance function. The value of this function at a point is the distance from that point to the interface. The level set function is updated by solving corresponding partial differential equations. A special reinitialization step is used to preserve properties of the level set function. Depending on the value of the level set function one may determine the subdomain as well as the position of the interface. The use of a smooth level set function makes it convenient to compute the normals to the interface and curvature. This is taken advantage of in two-phase flow problems with a surface tension force depending on the curvature of the interface [Chang *et al.* 1996]. This method has found many other applications

including solidification-melt dynamics, reacting flows [Sethian & Smereka 2003], computational geometry, modelling deposition of on material on another, modelling cell membranes, solidification of alloys [Gibou *et al.* 2018].

The level set method has clear advantages over other interface tracking methods. The smooth level set function allows to compute geometric quantities easily, it is easier to extend to higher dimensions, and it handles topological changes easily [Sethian & Smereka 2003]. The partial differential equations used to update the level set are conservation laws and have been studied well.

However, there has been a disadvantage of such methods: conservation of mass. Reinitialization steps, on the one hand and inaccurate numerical methods on the other, may disturb the mass conservation. This problem has been overcome in [Olsson & Kreiss 2005]. In this work using a conservative formulation and appropriate numerical methods along with an intermediate step that does not change the position of the interface a conservative level set method has been developed. The method has been further improved in [Olsson *et al.* 2007]. Instead of the distance function, a smoothed Heaviside function is used, which is equal to 0 in one subdomain 1 in the other. The interface is defined as the 0.5 level set and the level set function rapidly changes from 0 to 1 in a thin transition layer around the interface. Along with this a new reinitialization step, called the compression step is used. The compression step involves solving a partial differential equation to conserve the thickness of the interface layer. To initialize the new level set function, either an analytic solution of the compression step can be used, alternatively one may initialize the level set function to 1 in one subdomain and 0 in the other and run the compression step as proposed in [Olsson *et al.* 2007]. The method is shown to be conservative. Some theoretical developments on the properties of the scheme, like stability in the simplified one-dimensional case and conservation are provided.

Despite this, the scheme may become unstable in the points away from the interface. This happens due to the errors in the normal vector in the compression step, which strongly affect the direction of the unit normal vector in the regions where the level set function is approximately constant and equal to either 0 or 1. The issue can be worked around by calculating the normal vectors only near the interface. This problem has be addressed in more detail in [Zhao *et al.* 2014], where a second level set function is used to compute the normal vectors. Separate update and reinitialization steps are applied to the second level set function. An optimized approach is proposed in [Shervani-Tabar & Vasilyev 2018]. The compression step is modified to use a normal vector with norm one near the interface and diminishing magnitude away from the interface.

We use the method developed in [Olsson & Kreiss 2005] to describe our fluid-structure interface. It is especially useful since we consider incompressible flows. In the structure subdomain, the level set function is equal to 0, in fluid it is equal to 1, with a smooth transitional layer in between.

3.C Regularized formulation.

Using this level set method we can write the regularized formulation, from the equations obtained earlier 3.4 following the same idea as two-fluid interaction. We take advantage of the fact that both of these equations are formulated in the stress variables. We represent the fluid and structure subdomains of Ω using the level set function the following way:

$$\begin{cases} \phi > \dfrac{1}{2}, & \Omega^f; \\ \phi < \dfrac{1}{2}, & \Omega^s. \end{cases} \tag{3.6}$$

There will be three characteristic regions: $\phi = 0$, $\phi = 1$, $0 < \phi < 1$. The latter is transitional layer. Using the level set function ϕ, we first represent the new variable parameters regularizing density, viscosity and elasticity:

$$\begin{cases} \dfrac{1}{\rho_\phi} = \dfrac{\phi}{\rho^f} + \dfrac{1-\phi}{\rho^s}, \\ \dfrac{1}{\mu_\phi} = \dfrac{\phi}{\mu^f} + \dfrac{1-\phi}{\mu^s}. \end{cases} \tag{3.7}$$

Unlike interaction of two fluid phases, the problem 3.4 has different time derivatives. Thus we approximate the differential operators in time as follows (we will denote the regularized operator as ∂_ϕ):

$$\partial_\phi = \phi \partial_t + (1-\phi)\, \partial_{tt}. \tag{3.8}$$

With this preparation we can now formulate the regularized version of the problem in Ω:

$$\begin{cases} \dfrac{1}{\mu_\phi} \partial_\phi \left(A_{ijlm} \sigma_{lm} \right) - \partial_j \left(\dfrac{\partial_k \sigma_{ik}}{\rho_\phi} \right) - \partial_i \left(\dfrac{\partial_k \sigma_{jk}}{\rho_\phi} \right) \\ = \partial_j \left(\dfrac{f_i}{\rho_\phi} \right) + \partial_i \left(\dfrac{f_j}{\rho_\phi} \right); \\ \partial_t v_i - \dfrac{\partial_k \sigma_{ik}}{\rho_\phi} = \dfrac{f_i}{\rho_\phi}, \end{cases} \tag{3.9}$$

and with convection terms:

$$\begin{cases} \dfrac{1}{\mu_\phi} \partial_\phi \left(A_{ijlm} \tilde{\sigma}_{lm} \right) + \dfrac{1}{\mu_\phi} \partial_\phi \left(A_{ijlm} \rho_\phi v_l v_m \right) - \partial_j \left(\dfrac{\partial_k \tilde{\sigma}_{ik}}{\rho_\phi} \right) - \partial_i \left(\dfrac{\partial_k \tilde{\sigma}_{jk}}{\rho_\phi} \right) \\ = \partial_j \left(\dfrac{f_i}{\rho_\phi} \right) + \partial_i \left(\dfrac{f_j}{\rho_\phi} \right); \\ \partial_t v_i - \dfrac{\partial_k \tilde{\sigma}_{ik}}{\rho_\phi} = \dfrac{f_i}{\rho_\phi}, \end{cases} \tag{3.10}$$

These systems must be extended with the level set update equation:

$$\partial_t \phi + \partial_k \left(\phi v_k \right) = 0. \tag{3.11}$$

In numerical schemes that are used in practice, an intermediate step for the level set function ϕ is also used.

Chapter 4

The numerical scheme and results.

In this chapter we will use the previous results to derive the numerical scheme and discuss some practical issues. Finally we will present some benchmark results obtained using this scheme.

4.A Numerical scheme.

In this section, we will consider numerical schemes for systems 3.9 and 3.10. The numerical scheme for the level set method that is being used in this study is described in [Olsson & Kreiss 2005].

First we write the scheme discretized in time, using the time splitting proposed in [Minev & Vabishchevich 2018] and summarized in 2.A:

$$
\begin{cases}
\dfrac{1}{\mu_\phi^{n+1}}\delta_\phi \sigma_{12}^{n+1} - \left(\Delta_{22}^{n+1} + \Delta_{11}^{n+1}\right)\sigma_{12}^{n+1} - \Delta_{21}^{n+1}\sigma_{11}^{n} \\
- \Delta_{12}^{n+1}\sigma_{22}^{n} = \partial_2\left(\dfrac{f_1^{n+1}}{\rho_\phi^{n+1}}\right) + \partial_1\left(\dfrac{f_2^{n+1}}{\rho_\phi^{n+1}}\right); \\
\\
\dfrac{1}{\mu_\phi^{n+1}}\delta_\phi\left(\sigma_{11}^{n+1} - \sigma_{22}^{n+1}\right) - 4\Delta_{11}^{n+1}\sigma_{11}^{n+1} - 4\Delta_{12}^{n+1}\sigma_{12}^{n+1} \\
= 4\partial_1\left(\dfrac{f_1^{n+1}}{\rho_\phi^{n+1}}\right); \\
\\
\dfrac{1}{\mu_\phi^{n+1}}\delta_\phi\left(\sigma_{22}^{n+1} - \sigma_{11}^{n+1}\right) - 4\Delta_{22}^{n+1}\sigma_{22}^{n+1} - 4\Delta_{21}^{n+1}\sigma_{21}^{n+1} \\
= 4\partial_2\left(\dfrac{f_2^{n+1}}{\rho_\phi^{n+1}}\right);
\end{cases}
\tag{4.1}
$$

Here, $\delta_\phi = \frac{\phi}{\tau}\delta + \frac{1-\phi}{\tau^2}\delta^2$ and $\Delta_{ij}^{n+1} = \partial_i \frac{1}{\rho^{n+1}}\partial_j$.

For spatial discretization, we use the Marker and Cell (MAC) grid. Components of the velocity vector and external force vector are located on the corresponding faces of the grid cell. The off-diagonal components of stress are located on the vertex positions of the grid cell. The diagonal components of stress are located on the central positions of the grid cell. Suppose that the system is discretized the system on a uniform two-dimensional grid with step h in both directions, indices of vertex points are (l, m). We denote C_{ij}^{n+1} the discrete counterparts of operators Δ_{ij}^{n+1} and F_{ij}^{n+1} are discrete counterparts of $\partial_i\left(\frac{f_j^{n+1}}{\rho_\phi^{n+1}}\right)$. For example, for a discretized in space source term f_1^n which is located on face locations of the mac grid $(l, m+\frac{1}{2})$ we

have:

$$\begin{aligned}\left(F_{11}^{n+1}\right)_{l+\frac{1}{2},m+\frac{1}{2}} &= \frac{f_{1,l+1,m+\frac{1}{2}}^{n+1} - f_{1,l,m+\frac{1}{2}}^{n+1}}{h\rho_{\phi,l+\frac{1}{2},m+\frac{1}{2}}^{n+1}},\\ \left(F_{21}^{n+1}\right)_{l,m} &= \frac{f_{1,l,m+\frac{1}{2}}^{n+1} - f_{1,l,m-\frac{1}{2}}^{n+1}}{h\rho_{\phi,l,m}^{n+1}}.\end{aligned} \tag{4.2}$$

Other quantities F_{ij}^{n+1} are discretized a similar way. For operators C_{11}^{n+1}, C_{12}^{n+1} and a quantity $\psi_{l,m}$ located on vertices we have:

$$\begin{aligned}\left(C_{11}^{n+1}\psi\right)_{l,m} &= \frac{\psi_{l+1,m} - \psi_{l,m}}{h^2\rho_{\phi,l+\frac{1}{2},m}^{n+1}} - \frac{\psi_{l,m} - \psi_{l-1,m}}{h^2\rho_{\phi,l-\frac{1}{2},m}^{n+1}},\\ \left(C_{12}^{n+1}\psi\right)_{l+\frac{1}{2},m+\frac{1}{2}} &= \frac{\psi_{l+1,m+1} - \psi_{l+1,m}}{h^2\rho_{\phi,l+1,m+\frac{1}{2}}^{n+1}} - \frac{\psi_{l,m+1} - \psi_{l,m}}{h^2\rho_{\phi,l,m+\frac{1}{2}}^{n+1}}.\end{aligned} \tag{4.3}$$

For the same operators and for a quantity $\psi_{l+\frac{1}{2},m+\frac{1}{2}}$ located on central positions we have:

$$\begin{aligned}\left(C_{11}^{n+1}\psi\right)_{l+\frac{1}{2},m+\frac{1}{2}} &= \frac{\psi_{l+\frac{3}{2},m+\frac{1}{2}} - \psi_{l+\frac{1}{2},m+\frac{1}{2}}}{h^2\rho_{\phi,l+1,m+\frac{1}{2}}^{n+1}} - \frac{\psi_{l+\frac{1}{2},m+\frac{1}{2}} - \psi_{l-\frac{1}{2},m+\frac{1}{2}}}{h^2\rho_{\phi,l,m+\frac{1}{2}}^{n+1}},\\ \left(C_{12}^{n+1}\psi\right)_{l,m} &= \frac{\psi_{l+\frac{1}{2},m+\frac{1}{2}} - \psi_{l+\frac{1}{2},m-\frac{1}{2}}}{h^2\rho_{\phi,l+\frac{1}{2},m}^{n+1}} - \frac{\psi_{l-\frac{1}{2},m+\frac{1}{2}} - \psi_{l-\frac{1}{2},m-\frac{1}{2}}}{h^2\rho_{\phi,l-\frac{1}{2},m}}.\end{aligned} \tag{4.4}$$

The rest of the operators C_{ij}^{n+1} can be discretized in a similar way.

Once we discretize, the system 4.5 becomes:

$$
\begin{cases}
\dfrac{1}{\mu_\phi^{n+1}}\delta_\phi\sigma_{12}^{n+1} - \left(C_{22}^{n+1} + C_{11}^{n+1}\right)\sigma_{12}^{n+1} - C_{21}^{n+1}\sigma_{11}^{n} \\
- C_{12}^{n+1}\sigma_{22}^{n} = F_{21}^{n+1} + F_{12}^{n+1}; \\
\\
\dfrac{1}{\mu_\phi^{n+1}}\delta_\phi\left(\sigma_{11}^{n+1} - \sigma_{22}^{n+1}\right) - 4C_{11}^{n+1}\sigma_{11}^{n+1} - 4C_{12}^{n+1}\sigma_{12}^{n+1} = 4F_{11}^{n+1}; \\
\dfrac{1}{\mu_\phi^{n+1}}\delta_\phi\left(\sigma_{22}^{n+1} - \sigma_{11}^{n+1}\right) - 4C_{22}^{n+1}\sigma_{22}^{n+1} - 4C_{21}^{n+1}\sigma_{21}^{n+1} = 4F_{22}^{n+1};
\end{cases}
\tag{4.5}
$$

Now, expanding a rearranging the terms we get the following system

$$
\begin{cases}
\dfrac{1}{\mu_\phi^{n+1}\tau_\phi^{n+1}}\sigma_{12}^{n+1} - \left(C_{22}^{n+1} + C_{11}^{n+1}\right)\sigma_{12}^{n+1} = G_1^{n+1}; \\
\dfrac{1}{\mu_\phi^{n+1}\tau_\phi^{n+1}}\left(\sigma_{11}^{n+1} - \sigma_{22}^{n+1}\right) - 4C_{11}^{n+1}\sigma_{11}^{n+1} = G_2^{n+1}; \\
\dfrac{1}{\mu_\phi^{n+1}\tau_\phi^{n+1}}\left(\sigma_{22}^{n+1} - \sigma_{11}^{n+1}\right) - 4C_{22}^{n+1}\sigma_{22}^{n+1} = G_3^{n+1};
\end{cases}
\tag{4.6}
$$

with $\tau_\phi^{n+1} = \left(\frac{\phi^{n+1}}{\tau} + \frac{1-\phi^{n+1}}{\tau^2}\right)^{-1}$. The right hand sides are defined:

$$
\begin{aligned}
G_1^{n+1} =& F_{21}^{n+1} + F_{12}^{n+1} + C_{21}^{n+1}\sigma_{11}^{n} + C_{12}^{n+1}\sigma_{22}^{n} + \frac{\beta_\phi^{n+1}}{\mu_\phi^{n+1}}\sigma_{12}^{n} + \frac{\gamma_\phi^{n+1}}{\mu_\phi^{n+1}}\sigma_{12}^{n-1}; \\
G_2^{n+1} =& 4F_{11}^{n+1} + 4C_{12}^{n+1}\sigma_{12}^{n+1} + \frac{\beta_\phi^{n+1}}{\mu_\phi^{n+1}}\left(\sigma_{11}^{n} - \sigma_{22}^{n}\right) + \frac{\gamma_\phi^{n+1}}{\mu_\phi^{n+1}}\left(\sigma_{11}^{n-1} - \sigma_{22}^{n-1}\right); \\
G_3^{n+1} =& 4F_{22}^{n+1} + 4C_{21}^{n+1}\sigma_{21}^{n+1} + \frac{\beta_\phi^{n+1}}{\mu_\phi^{n+1}}\left(\sigma_{22}^{n} - \sigma_{11}^{n}\right) + \frac{\gamma_\phi^{n+1}}{\mu_\phi^{n+1}}\left(\sigma_{22}^{n-1} - \sigma_{11}^{n-1}\right);
\end{aligned}
\tag{4.7}
$$

with $\beta_\phi^{n+1} = \frac{\phi^{n+1}}{\tau} + 2\frac{1-\phi^{n+1}}{\tau^2}$ and $\gamma_\phi^{n+1} = -\frac{1-\phi^{n+1}}{\tau^2}$.

The off-diagonal system in 4.6 resembles a heat equation and are solved using direction splitting. This way one will need to solve only tri-diagonal systems of

linear equations. The diagonal system in 4.6 are solved together as one linear system with a left-hand side matrix with the following blocks:

$$\begin{pmatrix} \left(\frac{1}{\mu_\phi^{n+1}\tau_\phi^{n+1}}I - 4C_{11}^{n+1}\right) & -\frac{1}{\mu_\phi^{n+1}\tau_\phi^{n+1}}I \\ -\frac{1}{\mu_\phi^{n+1}\tau_\phi^{n+1}}I & \left(\frac{1}{\mu_\phi^{n+1}\tau_\phi^{n+1}}I - 4C_{22}^{n+1}\right) \end{pmatrix}, \tag{4.8}$$

where I represents the identity matrix. This system is solved using an iterative method with the following preconditioner:

$$\begin{pmatrix} \left(\frac{1}{\mu_\phi^{n+1}\tau_\phi^{n+1}}I - 4C_{11}^{n+1}\right) & 0 \\ -\frac{1}{\mu_\phi^{n+1}\tau_\phi^{n+1}}I & \left(\frac{1}{\mu_\phi^{n+1}\tau_\phi^{n+1}}I - 4C_{22}^{n+1}\right) \end{pmatrix}. \tag{4.9}$$

This preconditioner is easy to invert since one can solve the equations in the first row and use the result to solve for the second row. These solves involve tridiagonal matrices only.

In order to include the convection term into the system 4.6 we must modify the right-hand sides 4.7 adding the derivatives of $q_{ij} = A_{ijlm}\rho_\phi v_l v_m$:

$$\begin{aligned} \tilde{G}_1^{n+1} &= G_1^{n+1} - \frac{1}{\mu_\phi^{n+1}}\delta_\phi q_{12}^n; \\ \tilde{G}_2^{n+1} &= G_2^{n+1} - \frac{1}{\mu_\phi^{n+1}}\delta_\phi q_{11}^n; \\ \tilde{G}_3^{n+1} &= G_3^{n+1} - \frac{1}{\mu_\phi^{n+1}}\delta_\phi q_{22}^n. \end{aligned} \tag{4.10}$$

4.B Benchmark results.

4.B.1 Driven cavity with an elastic wall.

In this benchmark we simulate the lid-driven cavity flow in a 2×2 domain Ω with the bottom part 2×0.5 filled with a linear elastic solid Ω^s (Fig. 4.1). The setting is the same as described in [Zhao *et al.* 2008], [Dunne 2006]. The convection terms are omitted, we use the scheme 4.6. The fluid and structure constants are $\mu^f = \mu^s = 0.2$, $\rho^f = \rho^s = 1.0$. All the boundaries of the cavity have zero boundary condition for velocity except the top lid. At time 0 the top lid starts moving with the x component of velocity:

$$v_1 = \begin{cases} sin^2\left(\frac{\pi x}{6}\right), & x \in [0.0, 0.3]; \\ 1, & x \in (0.3, 1.7); \\ sin^2\left(\frac{\pi(x-2)}{6}\right), & x \in [1.7, 2.0]. \end{cases} \tag{4.11}$$

The domain is discretized by a uniform 100×100 grid. Initially, all the velocities are zero. As the cavity flow develops, the elastic bottom is deformed due to fluid-structure interaction. At time 2.5 the deformed level set is presented in Fig. 4.1, which is in agreement with the solution obtained in [Zhao *et al.* 2008].

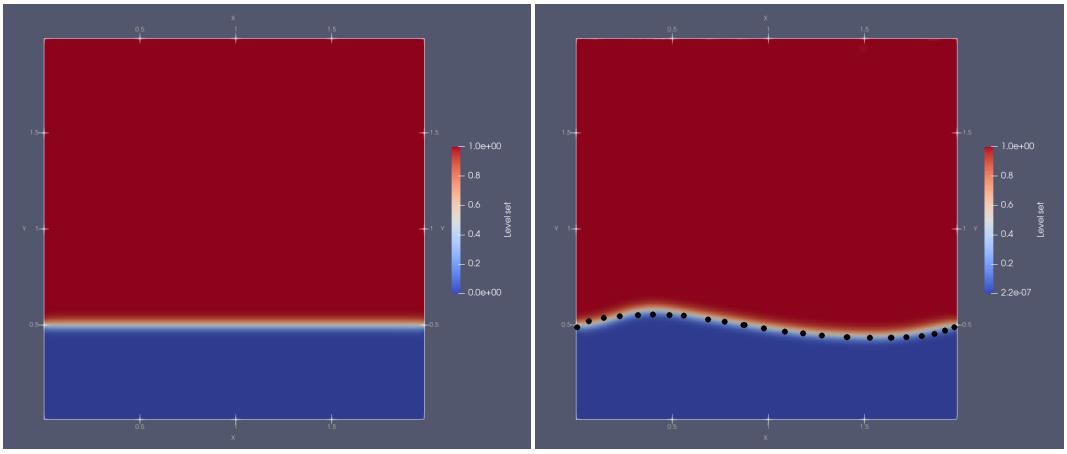

Figure 4.1: Lid driven cavity level set functions. Initial state (left) and final state (right). Black circles represent the solution obtained in [Zhao *et al.* 2008].

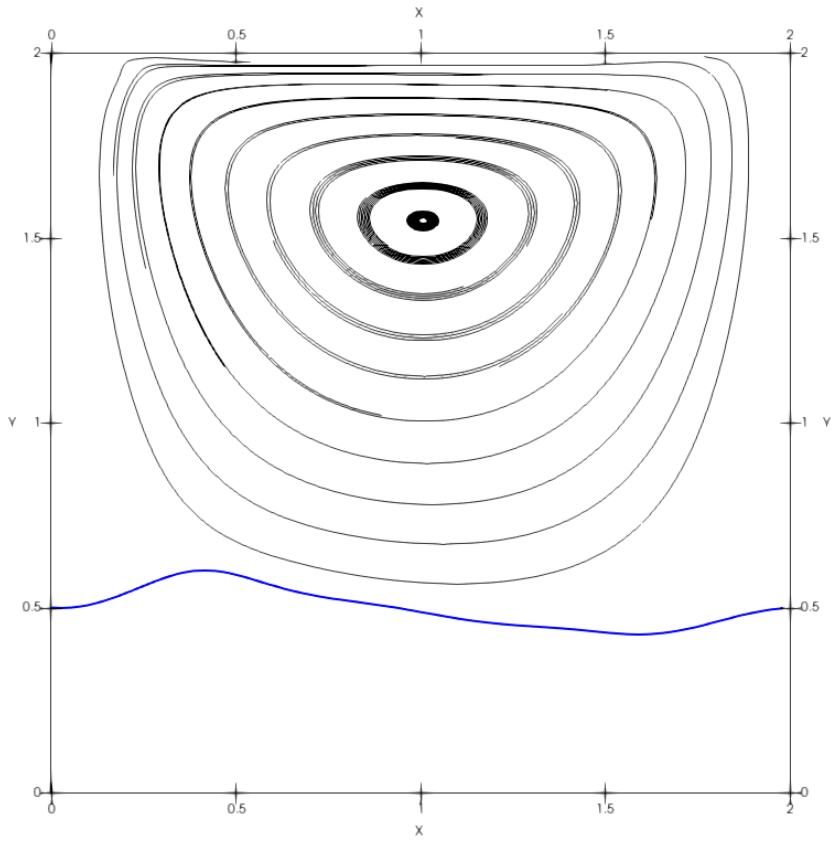

Figure 4.2: Lid driven cavity flow over the elastic solid, final state. The blue curve is 0.5 contour of the level set function.

The fluid streamlines are presented in Fig. 4.2.

4.B.2 Oscillating disk in fluid.

This is a modification of the oscillating disk benchmark presented in [Zhao *et al.* 2008]. An elastic disk with radius 0.1 is placed inside a 1×1 domain filled with fluid (Fig. 4.3). In the initial state all velocities are zero. Fluid and structure parameters are

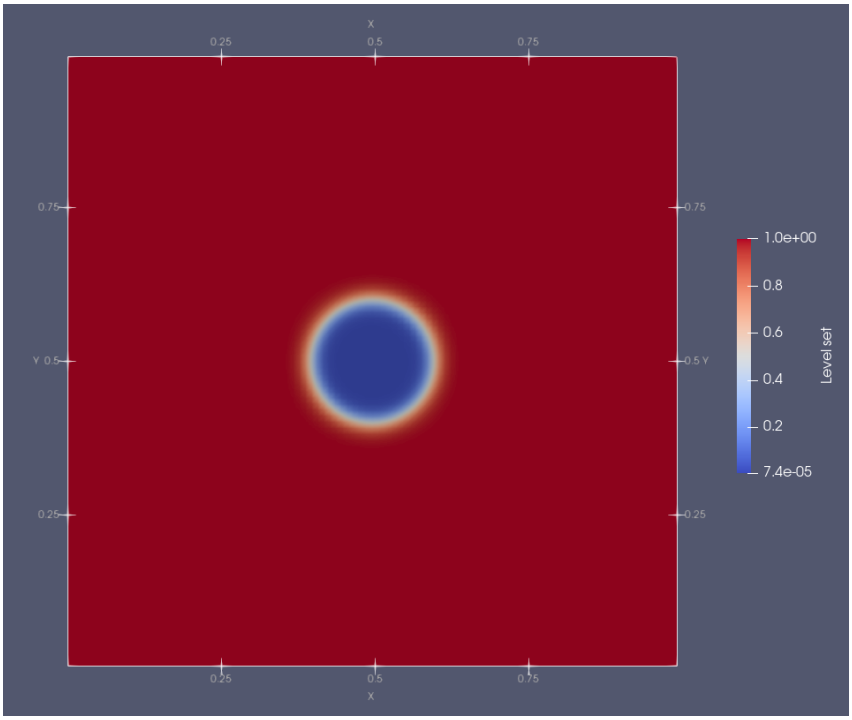

Figure 4.3: Oscillating disk, initial level set function.

$\rho^f = \rho^s = 0.1$, $\mu^f = 0.01$, $\mu^s = 0.05$. The boundary conditions for velocities are the following:

$$\begin{aligned} v_1 &= \frac{\pi}{5} c(t) sin(2\pi x) cos(2\pi y), \\ v_2 &= -\frac{\pi}{5} c(t) sin(2\pi y) cos(2\pi x). \end{aligned} \tag{4.12}$$

where $c(t)$ is defined as:

$$c(t) = \begin{cases} exp\left(1 - \dfrac{1}{1-(t-1)^2}\right), & t \in [0,1); \\ 1, & t \in [1,1.5); \\ 0, & t \in [1.5,3]. \end{cases} \tag{4.13}$$

The domain is discretized by a 100×100 uniform grid. The results are presented in Fig. 4.4, 4.6, 4.5.

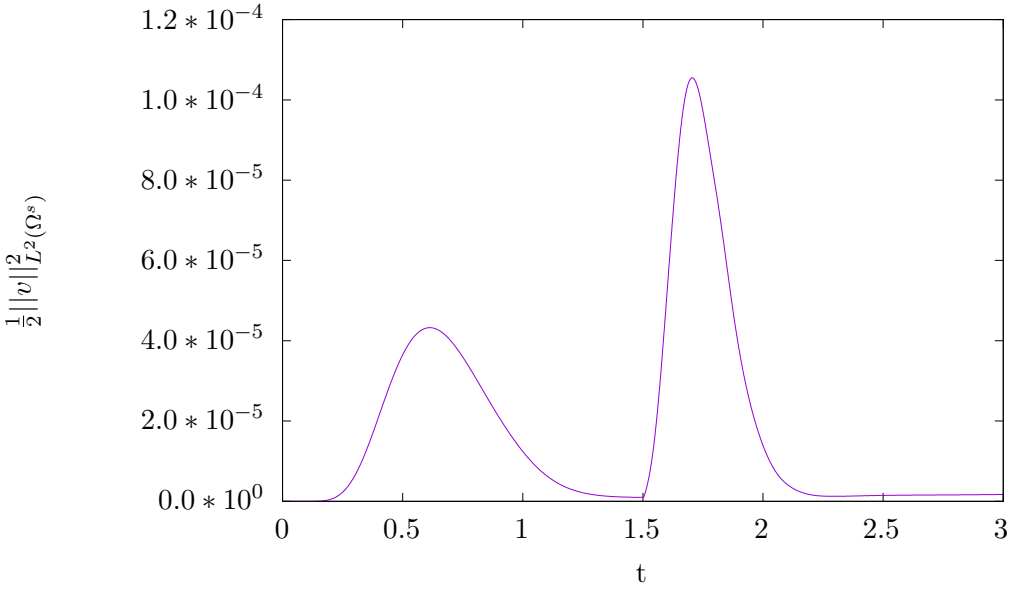

Figure 4.4: Oscillating disk. Norm of disk velocity over time.

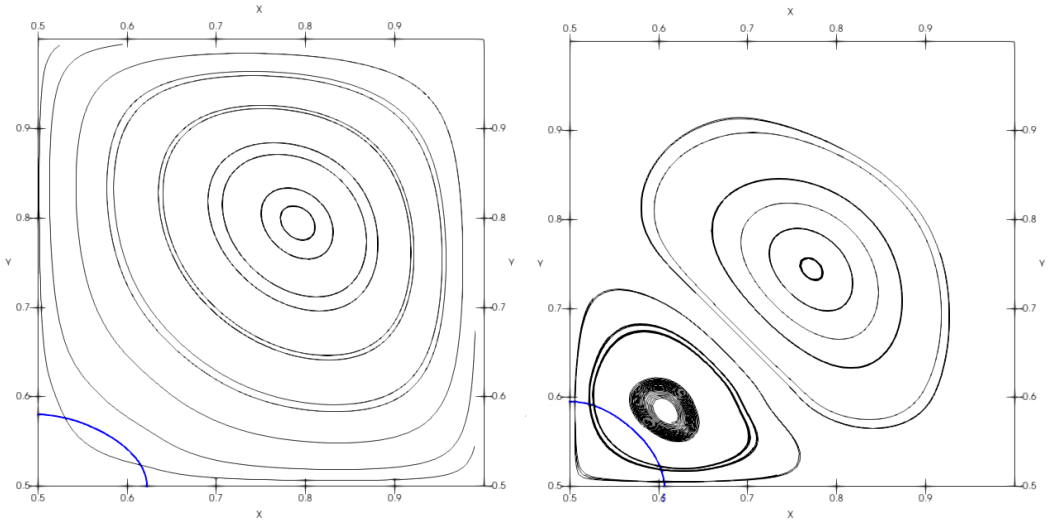

Figure 4.5: Streamlines at 0.975 (left) and 1.6 (right). The disk is denoted by the blue curve.

We start with a round disk and no fluid motion (Fig. 4.6 top left). As the boundary velocity increases, due to fluid structure interaction, the disk deforms (Fig. 4.6 top right, Fig. 4.5 left). The fluid friction forces are eventually compensated by forces of elasticity in the disk and the system comes to a stationary solution at $t = 1.5$, see (Fig. 4.4). As soon as the boundary velocity is set to zero at $t > 1.5$, the fluid friction is no longer compensated with elastic forces within the deformed disk, so the disk recoils back (Fig. 4.5 right). Although the original fluid motion continues by inertia between the disk and boundaries, the disk and fluid in its vicinity comes into motion. As a result of elastic forces and inertia in the disk, it recoils and deforms into an opposite extreme position (Fig. 4.6 bottom left.). Eventually, due to stresses in the disk, it comes into motion again and stops in the final state (Fig. 4.6 bottom right). Despite the different settings, the results are similar to the ones presented in [Zhao *et al.* 2008].

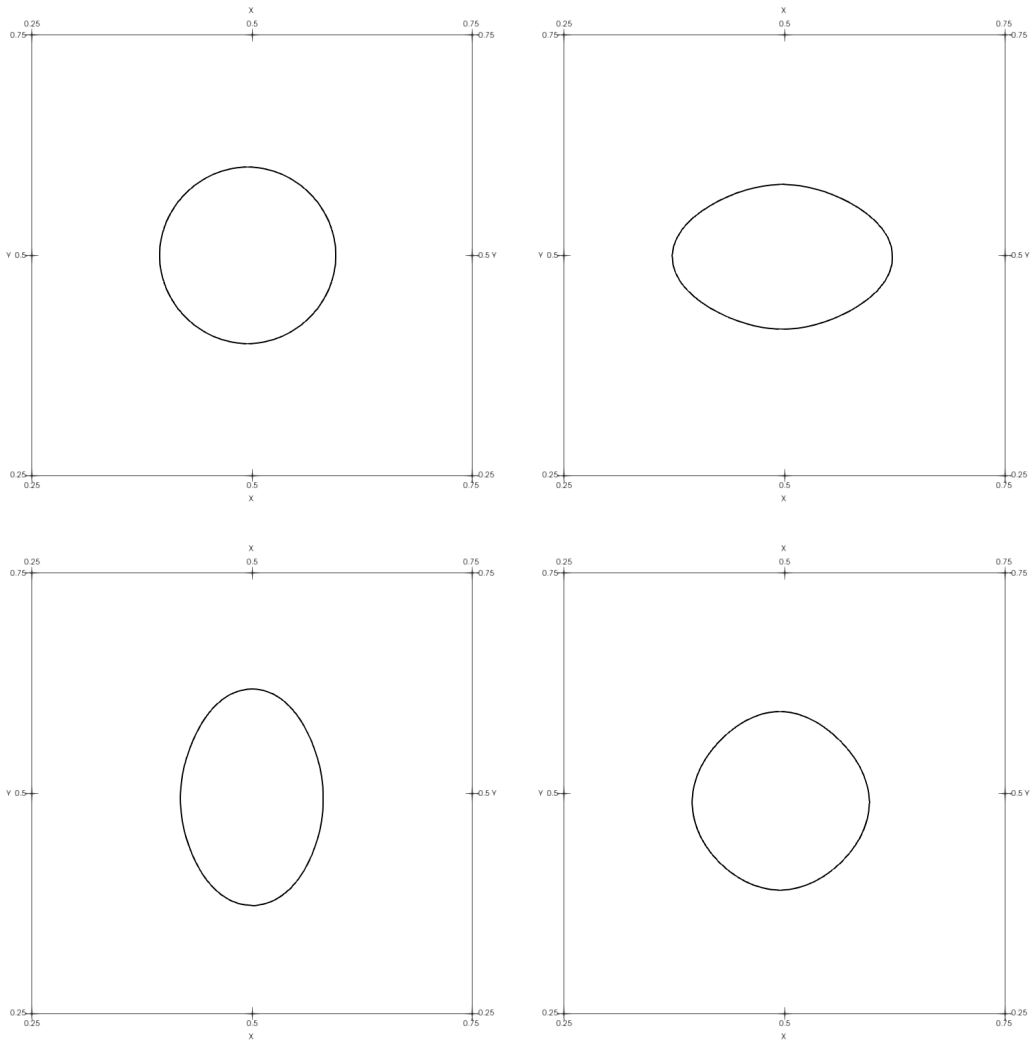

Figure 4.6: A 0.5 contour of the level set function at 0 (top left), 0.975 (top right), 2.0 (bottom left), 3.0 (bottom right).

Chapter 5

Conclusion

In this work, we have extended the stress formulation for linear structure and symmetric stress. Based on this formulation, we have developed a new method for FSI problems using the level set method. A numerical method with efficient solving strategies has been described. We have studied how this method compares to successful methods for FSI problems, proposed earlier. In the future, convective terms for fluid and structure can be included explicitly into the numerical scheme. It is also possible to extend the stress formulation and, as a consequence, this method to FSI with a Neo-Hookean non-linear stress tensor.

Bibliography

[Chang *et al.* 1996] Y. Chang, T. Hou, B. Merriman, & S. Osher, Journal of Computational Physics, **124**:449, 1996.

[Dunne & Rannacher 2006] T. Dunne & R. Rannacher, "Adaptive finite element approximation of fluid-structure interaction based on an eulerian variational formulation," in *Fluid-Structure Interaction*, edited by H.-J. Bungartz & M. Schäfer, pp. 110–145, Berlin, Heidelberg, 2006, Springer Berlin Heidelberg.

[Dunne 2006] T. Dunne, International Journal for Numerical Methods in Fluids, **51**:1017 , 2006.

[Gibou *et al.* 2018] F. Gibou, R. Fedkiw, & S. Osher, Journal of Computational Physics, **353**:82, 2018.

[Hoffman *et al.* 2011] J. Hoffman, J. Jansson, & M. Stöckli, Mathematical Models and Methods in Applied Sciences, **21**:491, 2011.

[Hou *et al.* 2012] G. Hou, J. Wang, & A. Layton, Communications in Computational Physics, **12**:337–377, 2012.

[Hron & Turek 2006] J. Hron & S. Turek, *A Monolithic FEM Solver for an ALE Formulation of Fluid-structure Interaction with Configuration for Numerical Benchmarking*, Ergebnisberichte angewandte Mathematik, Univ., 2006.

[Konovalov 1997] A. Konovalov, Sibirsk. Mat. Zh., **38**:551, 1997.

[Le Tallec & Mouro 2001] P. Le Tallec & J. Mouro, Computer Methods in Applied Mechanics and Engineering, **190**:3039, 2001, Advances in Computational Methods for Fluid-Structure Interaction.

[Legay *et al.* 2006] A. Legay, J. Chessa, & T. Belytschko, Computer Methods in Applied Mechanics and Engineering, **195**:2070, 2006.

[Minev & Vabishchevich 2018] P. Minev & P. N. Vabishchevich, Journal of Computational and Applied Mathematics, **344**:807, 2018.

[Olsson & Kreiss 2005] E. Olsson & G. Kreiss, Journal of Computational Physics, **210**:225, 2005.

[Olsson *et al.* 2007] E. Olsson, G. Kreiss, & S. Zahedi, Journal of Computational Physics, **225**:785, 2007.

[Osher & Sethian 1988] S. Osher & J. A. Sethian, Journal of Computational Physics, **79**:12, 1988.

[Peskin 1977] C. S. Peskin, Journal of Computational Physics, **25**:220, 1977.

[Sethian & Smereka 2003] J. A. Sethian & P. Smereka, Annual Review of Fluid Mechanics, **35**:341, 2003.

[Shervani-Tabar & Vasilyev 2018] N. Shervani-Tabar & O. V. Vasilyev, Journal of Computational Physics, **375**:1033, 2018.

[Sugiyama *et al.* 2017] K. Sugiyama, S. Ii, K. Shimizu, S. Noda, & S. Takagi, Procedia IUTAM, **20**:159, 2017, 24th International Congress of Theoretical and Applied Mechanics.

[Zhao *et al.* 2008] H. Zhao, J. B. Freund, & R. D. Moser, J. Comput. Phys., **227**:3114–3140, 2008.

[Zhao *et al.* 2014] L. Zhao, X. Bai, T. Li, & J. J. R. Williams, International Journal for Numerical Methods in Fluids, **75**:575, 2014.